Generalized switching function model of modular multilevel converter

G.P. Adam, P. Li, I.A. Gowaid and B.W. Williams
University of Strathclyde, Glasgow, UK
Email: grain.adam@strath.ac.uk

***Abstract*—this paper presents a generalized switching function model of the modular multilevel converter (MMC) that can be used instead of MMC electromagnetic transient simulation model for full-scale simulations of high-voltage dc (HVDC) and flexible ac transmission systems (FACTS). The proposed method is computationally more efficient and numerically stable than its electromagnetic transient simulation counterpart, and it is applicable for wide range of studies, including ac and dc network faults. The proposed switching function model is packaged in a graphical form to suit various simulation platforms such as Simulink and PSCAD. The validity of the presented model is confirmed using simulation and its scalability has been demonstrated on MMC with 301 cells per arm, considering power reversal during normal operation and dc short circuit fault.**

***Key words*—*electromagnetic transient simulation model; modular multilevel converter; high-voltage dc transmission systems; and switching function model*.**

I. INTRODUCTION

The increased uses of MMCs in voltage source converter based high-voltage dc (VSC-HVDC) transmission systems in recent years have made full-scale simulation of large ac/dc network increasingly challenging [1-9]. These have encouraged development of several MMC dynamic models that can be used for wide range of studies [1, 5, 10-20]. Amongst these models, MMC electromagnetic transient (EMT) simulation model discussed in [10, 16, 17] provides a viable way to simulate full-scale HVDC links that employ MMC with hundreds of cells per arm. References [10, 21] have demonstrated that the MMC EMT model can match its detailed switching counterpart in term of accuracy to microscopic levels, including during ac and dc network faults. However, high processing power demand of MMC EMT model may restrict its applications to detailed simulation studies such as protection and sizing of the converter active and passive components. MMC average models in [1, 5, 7, 13] are applicable for various dynamic studies, especially, in large power systems. References [14, 22] presented MMC switching function model that can be used for various state-state and dynamic studies and its experimental validation. Because the MMC models developed in [14, 22] rely on the use of complex state space equations, their generalization to MMC with N cells per arm are expected to be challenging and computationally inefficient due to large number of time variant matrices and differential equations to be solved. Also, severe cases such as ac and dc network faults are not considered.

This paper presents a simple and generic MMC switching function model suitable for wide range of studies, including ac and dc network fault. The presented MMC model is faster and computationally more efficient compared to MMC EMT models discussed in [10, 16, 17], as no matrices to be computed, and all numerical operations needed are collapsed to simple integrations, multiplications and additions. The validity of the presented model is demonstrated on full-scale model of MMC based HVDC converter stations, with 301 cells per arms, considering the cases of power reversal and dc fault. The presented model is validated against detailed switch model (where the power circuit is built using diode and insulated gate bipolar transistor (IGBT) from SIMPOWER Power Electronics Library of SIMULINK-MATLAB).

II. GENERALISED SWITCHING FUNCTION MODEL OF MODULAR MULTILEVEL CONVERTER

Fig. 1(a) shows one-phase leg of the modular multilevel converter with N cells per arm. Its proper operation requires the average voltage stress across each cell capacitor and switching must be maintained around V_{dc}/N. For phase '*a*', the output phase voltage 'v_{ao}' can be expressed in terms of upper arm cell capacitor voltages and positive pole-to-ground or lower arm cell capacitor voltages and negative pole-to-ground as:

$$v_{ao} = \tfrac{1}{2}V_{dc} - \sum_{J=1}^{N}\left(1-S_{uj}\right)v_{cj} - R_d i_{a1} - L_d \frac{di_{a1}}{dt} \qquad (1)$$

$$\text{or } v_{ao} = -\tfrac{1}{2}V_{dc} + \sum_{J=1}^{N}\left(1-S_{lj}\right)v_{cj} - R_d i_{a2} - L_d \frac{di_{a2}}{dt} \qquad (2)$$

Where, i_{a1} and i_{a2} are the upper and lower arm currents; V_{dc} is the pole-to-pole dc voltage; and R_d and L_d are resistance and inductance of the upper and lower arm reactors. The voltage across each arbitrary cell capacitor from the upper or lower arms of phase '*a*' for example can be expressed using switching function as:

$$\text{Upper arm: } v_{cj} = \frac{1}{C_m}\int\left(1-S_{uj}\right)i_{a1}(t)dt \qquad (3)$$

$$\text{Lower arm: } v_{cj} = \frac{1}{C_m}\int\left(1-S_{lj}\right)i_{a2}(t)dt \qquad (4)$$

The cell capacitor currents of the upper and lower are $i_{cj}(t) = \left(1-S_{uj}\right)i_{a1}(t)$ and $i_{cj}(t) = \left(1-S_{lj}\right)i_{a2}(t)$. Equations (1) to (4) can be repackaged to form graphical representation of the

MMC in Fig. 1(b); where, S_{uj} and S_{lj} represent the switch state of the main switch S_{aj} of the j^{th} cell from the upper and lower arms; and j is a natural number that varies from 1 to N. To mimic the typical MMC behaviour during dc faults, the back-to-back IGBTs are incorporated in each arm, with S_{A1} is kept permanently off while S_{A2} is kept on during normal operation and turned off during dc fault. Alternatively, the enhanced cell arrangement proposed in [21] can be adopted. Notice that the use of switched resistors in electromagnetic transient simulation approach discussed in [2, 10, 16, 17, 21] may lead to so called ill conductance matrices, which are difficult to invert and can cause numerical instability is some situation when explicitly defined fixed step trapezoidal integration method is used. Whilst the proposed switching function model does not require computation of matrix inverse at each time step, with its switching states vary between 1 and 0, instead of switched resistors in electromagnetic transient simulation model that vary between $10^{6}\Omega$ and $1^{-6}\Omega$. This makes the proposed switching function approach much numerically efficient and faster than its equivalent electromagnetic transient simulation model discussed in [2, 10, 16, 17, 21]. Therefore, the proposed MMC switching function model is expected to be attractive for detailed full-scale simulations of point-to-point and multi-terminal HVDC transmission systems.

.

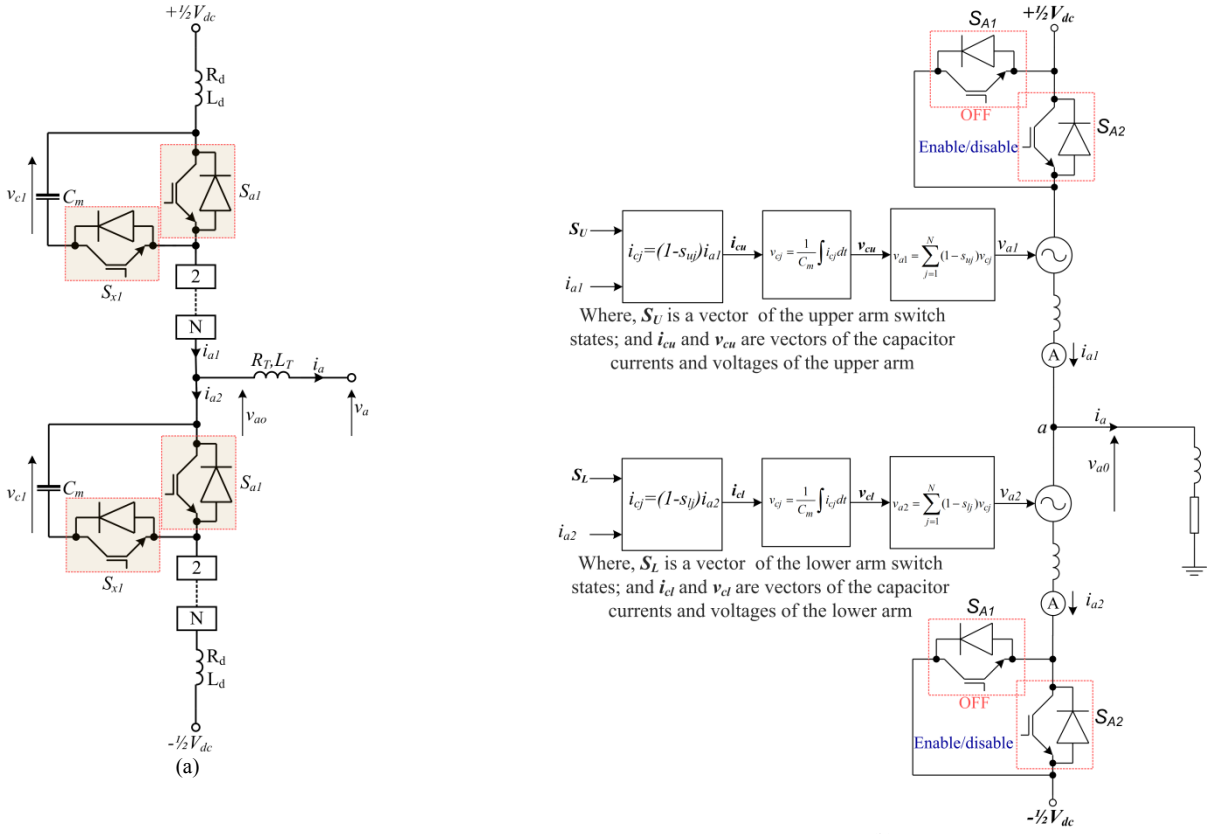

Fig. 1: (a) Generic representation of one-phase-leg of modular multilevel converter, and (b) graphical representation of generic MMC switching function model being proposed

III. OPEN LOOP DEMONSTRATION OF THE PROPOSED MODEL

A) Validation

This section validates the presented MMC switching function model against detailed switch model, considering the case of MMC with 21 cells per arm. Simulation results obtained from detailed switch model are superimposed on that obtained from the presented switching function model. In this validation, MMC input dc link voltage V_{dc}=*640kV*; modulation index m=*0.8*; arm inductance L_d=*30mH*; arm reactor internal resistance and total on-state resistance of the switching devices in each arm are lumped together in R_d=*0.25Ω*; cell capacitance C_m=*2mF*; and load resistance and inductance are 232.5Ω and 50mH per phase. Observe that all the selected waveforms in Fig. 2 obtained from both models are in full agreement to microscopic levels, including that for the phase output voltage, three-phase load currents, upper and lower arm currents and cell capacitor voltages. The validity of the presented switching function model is further confirmed by the percentage errors measured relative to detailed switch model plotted in Fig. 2 (e) to (g). Although Fig. 2 (g) displays larger instantaneous error, the average error is virtually zero.

B) Scalability

To demonstrate the scalability, simplicity and effectiveness of the presented MMC switching model as number of cells per arm increases, selected waveforms obtained from open loop operation of half-bridge MMC with 51 cells per arm are presented in Fig. 3. In this demonstration, all the MMC parameters remain the same as that in subsection (*A*), except the cell capacitance is increased to, C_m=5*mF*. Observe that the phase voltage (v_{ao}), three-phase load currents (i_a, i_b and i_c), upper and lower arm currents (i_{a1} and i_{a2}), and cell capacitor voltages in Fig. 3 are in line with that in Fig. 2, except the traces for the cell capacitor voltages as the number of cells per arm has changed. Notice that these results are achieved without any compromise to the accuracy compared to detailed switch and electromagnetic transient simulation models discussed in [10, 12, 17].

IV. FULL-SCALE SIMULATIONS

Fig. 4 shows a full-scale model of VSC-HVDC converter station that employs MMC with 301 cells per arm, with parameters listed in Table 1. The converter station in Fig. 4 is equipped with active and reactive power controller, inner current controller in d-q, and resonant controller for suppression of the 2nd harmonic currents in the MMC arms, and with modulator that uses amplitude modulation and Marquardt cell capacitor voltage balancing in the most inner loop. The power circuit is modelled using generalized switching function presented in Fig. 1(b).

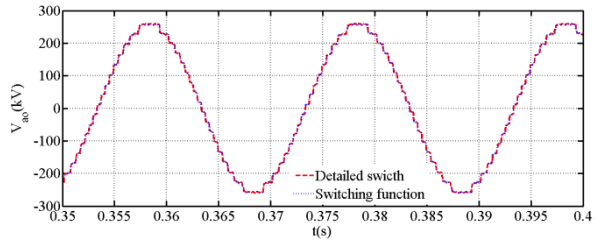

(a) Output phase voltage (V_{ao}, detailed switch superimposed on switching function)

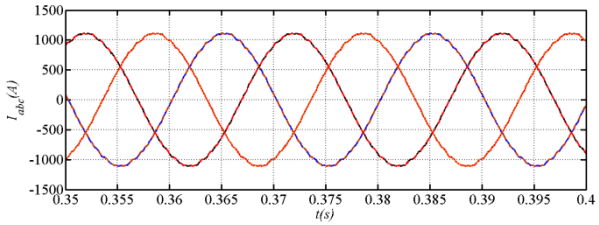

(b) Three-phase load currents (detailed switch superimposed on switching function)

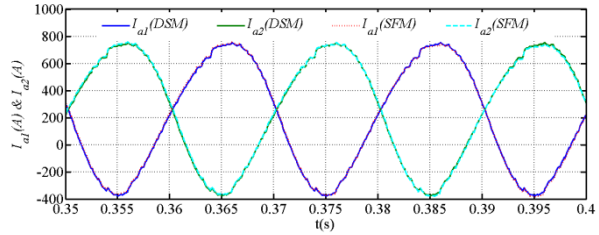

(c) Samples of upper and lower arm currents (phase a, detailed switch superimposed on switching function)

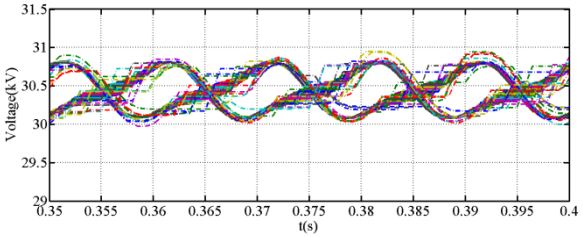

(d) Cell capacitor voltages (phase a, detailed switch superimposed on switching function)

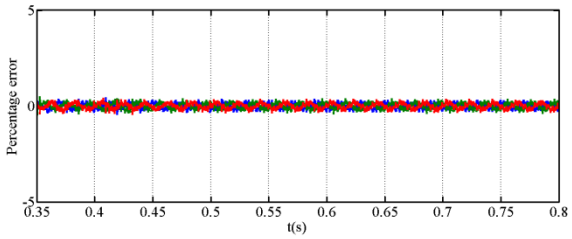

(e) Percentage error in the three-phase output currents (detailed switch versus switching function)

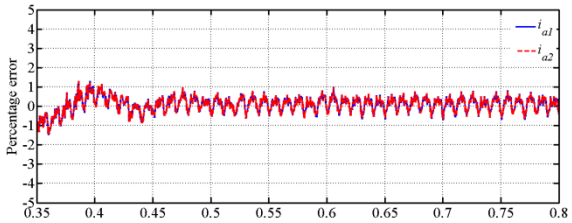

(f) Percentage error in the arm upper and lower arm currents (detailed switch versus switching function)

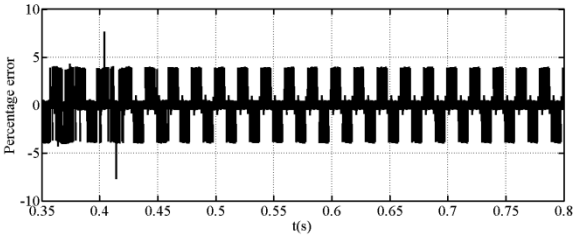

(g) Percentage error in the phase output voltage (detailed switch versus switching function)

Fig. 2: Validation of the presented switching function model against detailed switch model

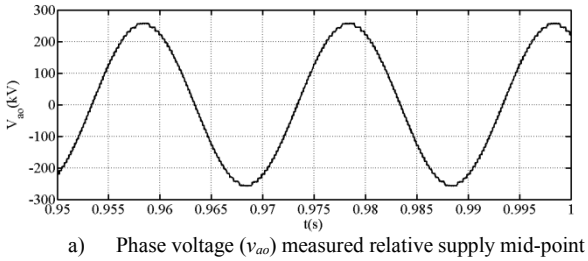

a) Phase voltage (v_{ao}) measured relative supply mid-point

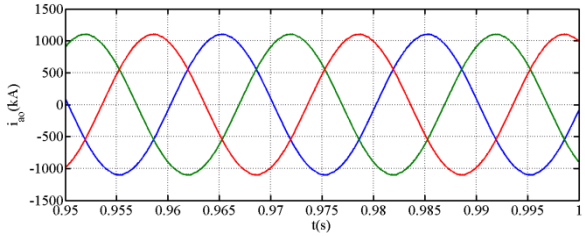

b) Three-phase load currents

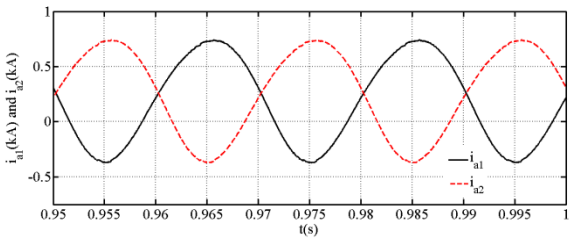

c) Sample of the upper and lower arm currents

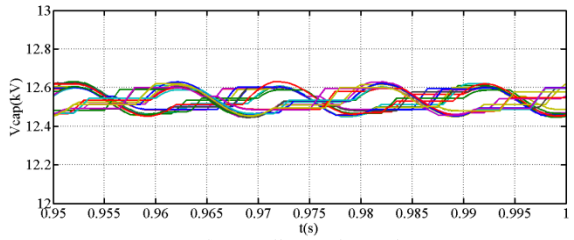

d) Cell capacitor voltages

Fig. 3: Waveforms illustrate the ability of the proposed model to reproduce the typical behaviour of half-bridge MMC during open loop (V_{dc}=*640kV*, modulation incex=0.8, number of cells per arm=51)

A) Normal operation

Fig. 5 shows simulation results obtained when converter station in Fig. 4 is initially commanded to inject 841MW with unity power factor into point of common coupling (PCC_1) at ac system 1, and at *t=0.8s,* the power flow is reversed to -841MW. Fig. 5(a) shows the MMC_1 presents a pure sinusoidal pre-filter ac voltage to low-voltage windings of its interfacing transformer as expected due to large number of cells per arms. Fig. 5(b) and (c) display active and reactive power MMC_1 exchanges with the ac system 1 at PCC_1 and corresponding arm currents. Observe that the 2nd harmonic current in each arm is successfully suppressed, and dc component of each arm current is varying with the magnitude and direction of the active power MMC_1 exchanges with PCC_1 (which is in line with the results shown in [10], using electromagnetic transient model). Fig. 5(d) shows that the MMC_1 cell capacitor voltages are tightly regulated around 2.1kVas anticipated. Besides, the plots for the switching device currents in Fig. 5 (e) and (f) show that the presented switching function model of the MMC being studied in this paper, is able to reproduce the current in MMC switching devices as in its detailed switching model and electromagnetic transient simulation equivalent[10]

Table 1: Summary of system parameters

Converter rating	1052MW
Rated active power	1000MW
Rated dc operating voltage	±320kV
Rated ac voltage	300kV
Number of cells per arm	301
Rated voltage per cell	2.126kV
Cell capacitance (C_m)	10mF
Inductance of arm reactor	15mH
Resistance of arm reactor	0.5Ω
Interfacing transformer rated power	1052MVA
Interfacing transformer voltage ratio	300kV/400kV
Interfacing transformer leakage inductance	0.2pu

B) DC fault

To examine the suitability of the presented generic MMC switching function model for dc fault studies, the HVDC converter station in Fig. 4 is subjected to a permanent pole-to-pole dc fault at *t=1s*, and gating signals to its switching devices are blocked immediately. Selected results obtained from the dc fault test stated above are displayed in Fig. 6. Plots for the converter station output currents, upper and lower arm currents (phase a) and switching devices currents (switches S_{a1} and S_{x1} of the first cell in the upper arm of phase a) in Fig. 6 (a), (b), (d) and (e) have shown that the presented switching function model is able to reproduce the typical behaviour of MMC during dc faults as detailed switch equivalent, including conduction of the switching devices when their gating signals are blocked. Fig. 6 (c) shows that the cell capacitor voltages remain flat as expected when converter switched are blocked during dc fault as diodes of the auxiliary switches that in series with cell capacitors tend to prevent the current flow from the ac side toward dc side through the cell capacitors, see Fig. 6 (e).

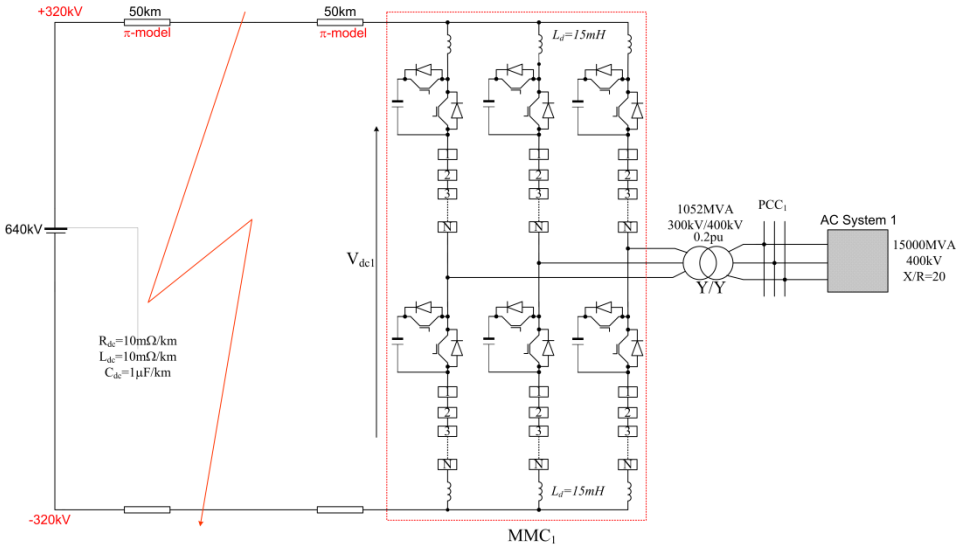

Fig. 4: Illustrate test system used to validate the proposed MMC switching function model

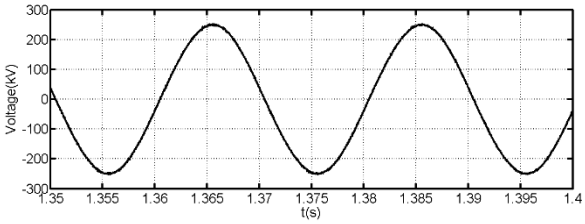

(a) Phase voltage measured at converter terminal

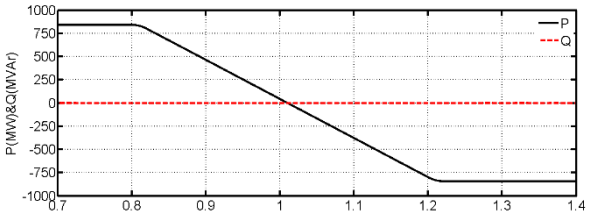

(b) Active and reactive power converter station exchanges with ac network at PCC_1

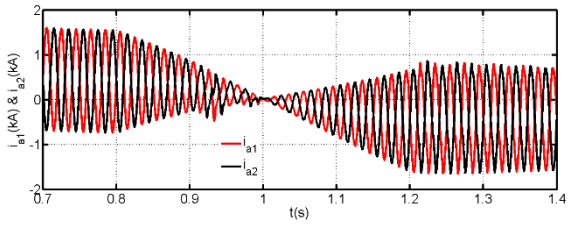

(c) Samples of the upper and lower arm currents (i_{a1} and i_{a2} of phase a)

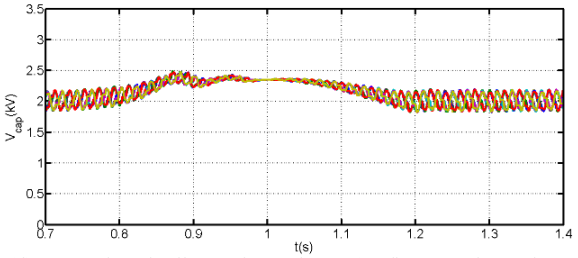

(d) Samples of cell capacitor voltages (10 first capacitor voltages from upper and lower arms of phase a)

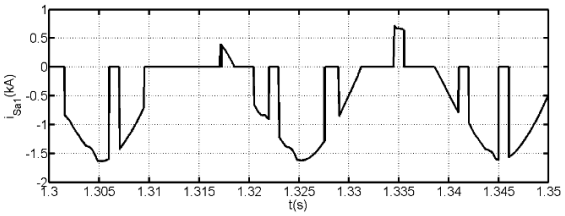

(e) Sample of current waveform in switch S_{a1} (first cell of phase a upper arm)

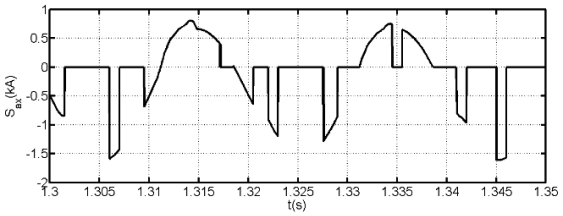

(f) Sample of current waveform in switch S_{x1} (first cell of phase a upper arm)

Fig. 5: Waveforms illustrating the capabilities of the proposed switching function based MMC model in capturing detailed behaviour of MMC during normal operation

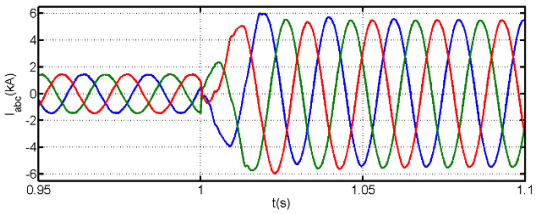

(a) Current waveforms MMC1 injects into PCC_1

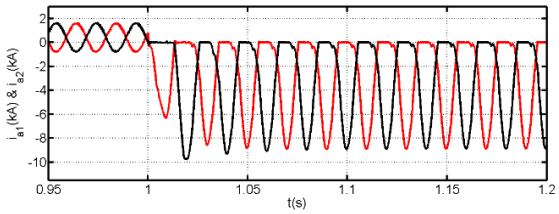

(b) Samples of the upper and lower arm currents (i_{a1} and i_{a2} of phase a)

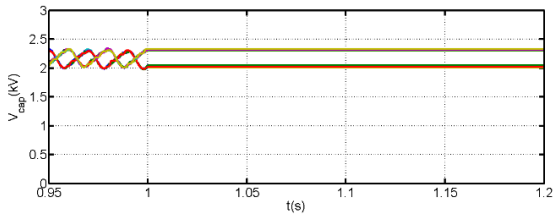

(c) Samples of cell capacitor voltages (10 first capacitor voltages from upper and lower arms of phase a)

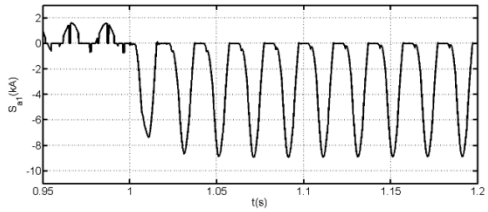

(d) Sample of current waveform in switch S_{a1} (first cell of phase a upper arm)

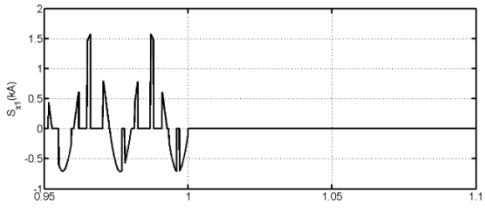

(e) Sample of current waveform in switch S_{x1} (first cell of phase a upper arm)

Fig. 6: Waveforms illustrating the capabilities of the proposed switching function based MMC model in capturing detailed behaviour of MMC during dc fault

V. CONCLUSIONS

This paper presented a generic switching function model for the half-bridge modular multilevel converter that can be used instead of detailed switched and electromagnetic transient simulation models when simulating full-scale HVDC transmission systems, with hundreds of cells per arm. The presented model has validated against switching model and its viability has been demonstrated in open and closed loop operations, including its scalability. Simulation studies presented in this paper have shown that the presented MMC model is able to capture detailed behaviour of the typical modular multilevel converter to microscopic levels. Furthermore, the presented MMC model is numerically stable and computational efficient compared to its EMT counterpart. The same modelling approach can be extended to full-bridge MMC and other hybrid multilevel converters.

VI. REFERENCES

[1] D. C. Ludois and G. Venkataramanan, "Simplified Terminal Behavioral Model for a Modular Multilevel Converter," *Power Electronics, IEEE Transactions on,* vol. 29, pp. 1622-1631, 2014.

[2] L. Sheng, X. Zheng, H. Wen, T. Geng, and X. Yinglin, "Electromechanical Transient Modeling of Modular Multilevel Converter Based Multi-Terminal HVDC Systems," *Power Systems, IEEE Transactions on,* vol. 29, pp. 72-83, 2014.

[3] G. J. Kish, C. Holmes, and P. W. Lehn, "Dynamic modeling of modular multilevel DC/DC converters for HVDC systems," in *Control and Modeling for Power Electronics (COMPEL), 2014 IEEE 15th Workshop on*, 2014, pp. 1-7.

[4] B. S. Riar and U. K. Madawala, "Modelling of modular multilevel converter topology with voltage correcting modules," in *Power Electronics for Distributed Generation Systems (PEDG), 2014 IEEE 5th International Symposium on*, 2014, pp. 1-4.

[5] M. Sleiman, A. Al Hage Ali, H. F. Blanchette, K. Al-Haddad, B. Piepenbreier, and H. Kanaan, "A survey on modeling, control, and dc-fault protection of modular multilevel converters for HVDC systems," in *Industrial Electronics (ISIE), 2014 IEEE 23rd International Symposium on*, 2014, pp. 2149-2154.

[6] G. Deiml, C. Hahn, W. Winter, and M. Luther, "A novel dynamic model for Multiterminal HVDC systems based on self-commutated full- and half-bridge Multilevel Voltage Sourced Converters," in *Power Electronics and Applications (EPE'14-ECCE Europe), 2014 16th European Conference on*, 2014, pp. 1-13.

[7] W. Jun, E. Farr, R. Burgos, D. Boroyevich, R. Feldman, A. Watson*, et al.*, "State-space switching model of modular multilevel converters," in *Control and Modeling for Power Electronics (COMPEL), 2013 IEEE 14th Workshop on*, 2013, pp. 1-10.

[8] W. Z. El-Khatib, J. Holboell, and T. W. Rasmussen, "Efficient modelling of a modular multilevel converter," in *Power Engineering Conference (UPEC), 2013 48th International Universities'*, 2013, pp. 1-6.

[9] M. Sztykiel, R. Da Silva, R. Teodorescu, L. Zeni, L. Helle, and P. C. Kjaer, "Modular multilevel converter modelling, control and analysis under grid frequency deviations," in *Power Electronics and Applications (EPE), 2013 15th European Conference on*, 2013, pp. 1-11.

[10] G. P. Adam and B. W. Williams, "Half and Full-Bridge Modular Multilevel Converter Models forSimulations of Full-Scale HVDC Links and Multi-terminal DC grids," *Emerging and Selected Topics in Power Electronics, IEEE Journal of,* vol. PP, pp. 1-1, 2014.

[11] G. P. Adam, S. J. Finney, K. H. Ahmed, and B. W. Williams, "Modular multilevel converter modeling for power system studies," in *Power Engineering, Energy and Electrical Drives (POWERENG), 2013 Fourth International Conference on*, 2013, pp. 1538-1542.

[12] H. Saad, Dennetie, x, S. re, J. Mahseredjian, P. Delarue*, et al.*, "Modular Multilevel Converter Models for Electromagnetic Transients," *Power Delivery, IEEE Transactions on,* vol. 29, pp. 1481-1489, 2014.

[13] M. A. Perez, S. Bernet, J. Rodriguez, S. Kouro, and R. Lizana, "Circuit Topologies, Modeling, Control Schemes, and Applications of Modular Multilevel Converters," *Power Electronics, IEEE Transactions on,* vol. 30, pp. 4-17, 2015.

[14] J. Wang, R. Burgos, and D. Boroyevich, "Switching-Cycle State-Space Modeling and Control of the Modular Multilevel Converter," *Emerging and Selected Topics in Power Electronics, IEEE Journal of,* vol. PP, pp. 1-1, 2014.

[15] H. Saad, J. Peralta, S. Dennetiere, J. Mahseredjian, J. Jatskevich, J. A. Martinez*, et al.*, "Dynamic Averaged and Simplified Models for MMC-Based HVDC Transmission Systems," *Power Delivery, IEEE Transactions on,* vol. 28, pp. 1723-1730, 2013.

[16] X. Jianzhong, Z. Chengyong, L. Wenjing, and G. Chunyi, "Accelerated Model of Modular Multilevel Converters in PSCAD/EMTDC," *Power Delivery, IEEE Transactions on,* vol. 28, pp. 129-136, 2013.

[17] U. N. Gnanarathna, A. M. Gole, and R. P. Jayasinghe, "Efficient Modeling of Modular Multilevel HVDC Converters (MMC) on Electromagnetic Transient Simulation Programs," *Power Delivery, IEEE Transactions on,* vol. 26, pp. 316-324, 2011.

[18] J. Xu, A. M. Gole, and C. Zhao, "The Use of Averaged-Value Model of Modular Multilevel Converter in DC Grid," *Power Delivery, IEEE Transactions on,* vol. PP, pp. 1-1, 2014.

[19] M. Heidari, S. Filizadeh, and A. M. Gole, "Electromagnetic Transients Simulation-Based Surrogate Models for Tolerance Analysis of FACTS Apparatus," *Power Delivery, IEEE Transactions on,* vol. 28, pp. 797-806, 2013.

[20] W. Leterme and D. Van Hertem, "Reduced modular multilevel converter model to evaluate fault transients in DC grids," in *Developments in Power System Protection (DPSP 2014), 12th IET International Conference on*, 2014, pp. 1-6.

[21] F. B. Ajaei and R. Iravani, "Enhanced Equivalent Model of the Modular Multilevel Converter," *Power Delivery, IEEE Transactions on,* vol. PP, pp. 1-1, 2014.

[22] S. Rohner, J. Weber, and S. Bernet, "Continuous model of Modular Multilevel Converter with experimental verification," in *Energy Conversion Congress and Exposition (ECCE), 2011 IEEE*, 2011, pp. 4021-4028.